Potential predictability of the Madden-Julian Oscillation in a superparameterizated model

Sarah Weidman [1], **Zhiming Kuang** [1,2]

[1]Department of Earth and Planetary Sciences, Harvard University, Cambridge, MA, USA
[2]John A. Paulson School of Engineering and Applied Sciences, Harvard University, Cambridge, MA, USA

Key Points:

- A novel approach is used to conduct perfect-model predictability experiments using a superparameterized global model.
- A single ensemble member model with superparameterized convection finds a potential Madden-Julian Oscillation predictability of 35-40 days.
- Resulting predictability estimates are comparable to those from current state-of-the-art multiple ensemble member forecasting models.

Corresponding author: Sarah Weidman, `sweidman@g.harvard.edu`

Abstract

The Madden-Julian Oscillation (MJO) is a promising target for improving sub-seasonal weather forecasts. Current forecast models struggle to simulate the MJO due to imperfect convective parameterizations and mean state biases, degrading their forecast skill. Previous studies have estimated a potential MJO predictability 5-15 days higher than current forecast skill, but these estimates also use models with parameterized convection. We perform a perfect-model predictability experiment using a superparameterized global model, in which the convective parameterization is replaced by a cloud resolving model. We add a second "silent" cloud resolving component to the control simulation that independently calculates convective-scale processes using the same large-scale forcings. The second set of convective states are used to initialize forecasts, representing uncertainty on the convective scale. We find a potential predictability of the MJO of 35-40 days in boreal winter using a single-member ensemble forecast.

Plain Language Summary

The Madden-Julian Oscillation is a convective signal in the tropics that has the potential to improve 10-40-day weather forecasts. Current weather forecast models struggle to simulate the MJO, leading to a lower forecast skill than many studies estimate could be possible. We use a model with a comparatively good representation of the MJO that uses a cloud permitting model to calculate convection information and modify its structure to generate MJO forecasts of its own MJO. Results from these forecasts suggest that the MJO in this model could be predictable up to 35-40 days using a single-member ensemble forecast, which is 5-10 days longer than current state-of-the-art ensemble forecasts.

1 Introduction

The Madden-Julian Oscillation (MJO) is a quasi-periodic signal of eastward propagating convection anomalies in the tropics with a period of 30-60 days (Madden & Julian, 1971, 1972). Active MJO events occur on an irregular basis, though most commonly during October - April, and vary considerably between events by their individual propagation, amplitude, and life cycle characteristics (B. Wang et al., 2019). As the dominant form of intraseasonal variability in the tropics, the MJO strongly impacts precipitation timing and amounts over the Maritime Continent, but it has also been connected to tropical cyclone activity (e.g., Vitart & Robertson, 2018), midlatitude weather (e.g., Sardeshmukh & Hoskins, 1988; Henderson et al., 2016; Arcodia et al., 2020), and many other aspects of global atmospheric circulation.

The timescale, quasiperiodic nature, and widespread impacts of the MJO make it a promising target for improving subseasonal weather forecasts (Waliser et al., 2003). Ample research and model development efforts have recently been delegated towards improving weather forecast model prediction skill of the MJO and its teleconnections (Vitart, 2017; H. Kim et al., 2018), resulting in a prediction skill of around 30 days for some weather forecast models (Xiang et al., 2022; Zavadoff et al., 2023; Peng et al., 2023). However, models face significant challenges when trying to simulate and forecast the MJO. For one, the MJO is a convective signal, but most forecast models must parameterize convection due to their coarse resolution, leading to errors in simulating MJO propagation, initiation, and amplitude (H. Zhu et al., 2009; H. Kim et al., 2019). Simulation of the MJO is further degraded by mean state biases that hamper their MJO simulation, including biases in mean moisture gradient, SST variability, and horizontal moisture advection (H. Kim et al., 2019; Kang et al., 2020; Lim et al., 2018). All of these issues interact in complex ways to limit MJO forecast skill.

Poor model representation of the MJO prompts the question of how predictable the MJO could be, if models were improved. Previous studies address this question using perfect-model predictability experiments, exemplified in Waliser et al. (2003). In these experiments, instead of computing skill using model forecast errors from observations, the observations are replaced by another simulation from the same model as the forecasts. These experiments can be considered a "best case scenario" for prediction skill if the forecast model had a perfect mean state and near-perfect initial conditions (H. Kim et al., 2018). Previous perfect-model predictability experiments found a potential MJO predictability of up to 35-45 days when using state-of-the-art ensemble forecast models (Neena et al., 2014; Xiang et al., 2022; S. Wang et al., 2019; Wu et al., 2016).

Most predictability estimates use coarse resolution models that parameterize convection. J. Zhu et al. (2020) showed that the potential predictability of the MJO is strongly dependent on convective parameterization scheme, with a more realistic (though still imperfect) scheme being more predictable by up to 15 days. The impressive 35-40-day MJO predictability in ECMWF ensemble forecasts (S. Wang et al., 2019) has been attributed to improvements in convective paramterization and model physics (Vitart, 2014), though the ECMWF still uses a parameterization for convection. Further, the literature varies substantially in how they generate initial conditions for the forecasts runs, which clouds the interpretability of potential predictability estimates from multi-model forecasts (Vitart, 2017).

An alternative to using a convective parameterization is to simulate the MJO in fine resolution, global cloud-permitting models (Miyakawa et al., 2014; Zavadoff et al., 2023). The MJO in these models is more realistic and yields prediction skill of nearly 30 days with a single ensemble forecast (comparable to an 11-member ensemble ECMWF forecast). However, these models are extremely computationally expensive and can only feasibly simulate comparatively few MJO events (< 100 in the above studies), restricting their ability to assess the potentially significant differences in predictability for different MJO characteristics and background states (Wu et al., 2023). A more computationally practical alternative is to use a multiscale modeling framework that couples a coarse resolution global model to a fine resolution cloud resolving model (Randall et al., 2016; Hannah et al., 2015). These multiscale models are much more efficient than global cloud permitting models, and the multiscale framework naturally permits separating convective vs. large scale influence on predictability. As yet, no studies have used a multiscale model to extensively estimate MJO potential predictability.

In this manuscript, we perform a perfect-model predictability experiment using a superparameterized version of CAM (SPCAM), a multiscale model that replaces the convective parameterization in CAM with a cloud resolving component. We utilize the multiscale structure of superparameterization to generate initial conditions for the forecast runs by imposing a perturbation on the convective scale. Section 2 describes the model and initial condition generation procedure, then defines the analyses used for estimating predictability. Section 3 shows the results of the predictability experiments, and Section 4 discusses the results in context of previous work and their limitations.

2 Methods

2.1 Model and initial conditions

We assess the potential predictability of the MJO using a superparameterized version of the Community Atmospheric Model (SPCAM) (M. F. Khairoutdinov & Randall, 2001; M. Khairoutdinov et al., 2005). The global climate model (GCM) component of SPCAM is CAM4 with 1.9°latitude x 2.5°longitude resolution, 26 vertical levels, and a timestep of 30 minutes. Sea surface temperatures are prescribed using monthly climatology. Each larger GCM-scale grid box has a 2-D cloud resolving model (CRM) embedded within it. The CRM calculates the cloud-scale processes explicitly, replacing the convective parameterization. Each CRM has 32 horizontal gridboxes aligned east to west in each larger GCM gridbox, with 4000m horizontal resolution and 24 vertical levels that align with the lower levels of the GCM. The CRM timestep is 20 seconds. The CRMs use a one-moment SAM microphysics parameterization scheme based on M. F. Khairoutdinov and Randall (2003). The CRMs are running simultaneously with the GCM but at a shorter timestep; large-scale tendencies from the GCM and convective-scale tendencies from the CRMs are passed between the models at each GCM timestep.

SPCAM has been shown to simulate a propagating MJO relatively well. Benedict and Randall (2009) and M. Khairoutdinov et al. (2008) describe some of the main improvements and lingering biases of SPCAM, which we summarize here. SPCAM reasonably simulates the observed wavenumber-frequency spectrum of subseasonal tropical waves, including the MJO. The general structural evolution and geographic span of the MJO is well represented in SPCAM. The main bias of SPCAM is that it overestimates the strength and variability of the MJO, especially over the Western Pacific, in opposition to most GCMs that have a weak MJO.

To generate initial conditions for the forecast runs, we add a second CRM to each GCM gridbox in SPCAM, following the idea of "multiple-instance superparameterization" in Subramanian and Palmer (2017); Jones et al. (2019). During the control simulation, we modify the radiative and convective components of SPCAM to run a second "silent" CRM in parallel to the standard CRM in each gridbox. See Figure 1 as a visual guide. At each timestep, the GCM passes the same large-scale information to both CRMs. Each CRM independently calculates convective tendencies as in regular SPCAM, but only the first CRM passes information back to the GCM. The second "silent" CRM simply outputs its state to a file. Each CRM uses CRM-scale information from its own previous timestep and thus stays spun up throughout the simulation. The GCM only receives information from one continuous CRM, so the control run output is essentially a standard SPCAM simulation. Each CRM is initialized by a random temperature perturbation near the surface on the first timestep; afterwards, they run continuously and independently.

The second silent CRM information is used as the initial perturbation for the forecast runs. The GCM-scale information used in the forecast restarts is the same as from the control run, so the only initial perturbation of the forecast is from the convective scale. This allows for scale separation of the initial perturbation and can be thought of as simulating a situation where we have perfect information of the GCM-scale conditions with uncertainty in the convective scale. Subramanian and Palmer (2017); Jones et al. (2019) examined how running multiple CRM components affects ensemble spread and found the stochastic-like nature of the CRMs better represents observed variance of deep convection in the tropics than convective parameterizations.

For this project, we use a 20-year control simulation. 60-day single ensemble member forecasts are restarted using the silent CRM information in a regular version of SPCAM every 5 days during boreal winter (October - April), resulting in 798 forecasts.

2.2 Analyzing predictability

To isolate the MJO signal from our forecast runs, we use a version of the OLR-based MJO index (OMI), first developed in Kiladis et al. (2014) and modified in Weidman et al. (2022). The OMI is an EOF-based index that uses the two leading principal components (PCs) of 30-96-day filtered daily tropical OLR to track the strength and propagation of the MJO through time. For forecasting purposes, we use a real-time version of the OMI (ROMI) as described in Kiladis et al. (2014); S. Wang et al. (2019). In brief, the ROMI is calculated by removing the mean OLR anomaly of the previous 40 days from the raw OLR anomaly and then taking a 9-day running average of the result, tapered

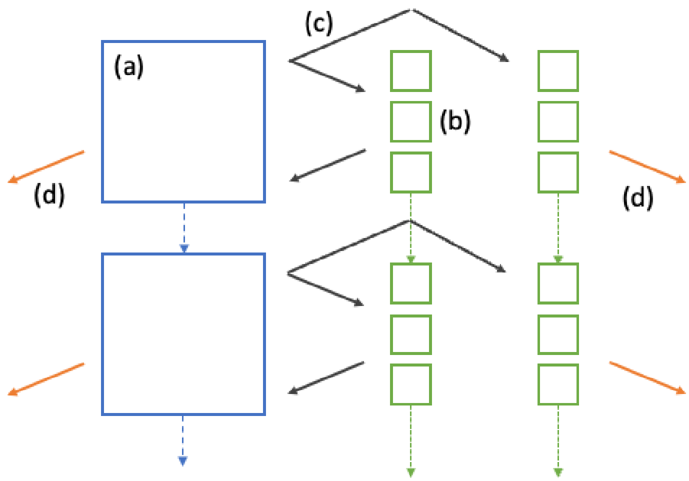

Figure 1. Schematic of silent CRM during control simulation. Large boxes (a) represent the GCM grid. The two columns of green boxes (b) represent the grids of the two CRMs. Each CRM has an east-west dimension of 32 per GCM gridbox in the simulation. The GCM passes large-scale information to both CRMs, but only the left CRM passes information back to the GCM, represented by black arrows (c). Orange arrows (d) denote the GCM and the silent CRM saving information for restarting the forecast runs.

to 7-, 5-, 3-, and 1-day running averages at the end of the forecast. This is to remove high and low frequency signals beyond that of the MJO. The filtered/smoothed OLR is then projected onto a set of seasonally-varying OLR-based EOFs calculated from an independent 40-year SPCAM run, following the EOF rotation procedure in Weidman et al. (2022). The OLR anomaly is calculated by removing the mean and first 3 harmonics of the seasonal cycle from each gridpoint, again calculated from a 40-year SPCAM run.

Many studies use the real-time multivariate (RMM) index (Wheeler & Hendon, 2004) for forecasting purposes. The RMM is based on EOFs describing the zonal structure of OLR and zonal wind at 200 and 850 hPa; however, Straub (2013) showed that the RMM underrepresents convection compared to zonal wind, causing the RMM to miss MJO-like convective signals and poorly predict desired forecasting variables such as precipitation and surface temperature (S. Wang et al., 2019; Kumar et al., 2020; Hannah et al., 2015). In addition, the lack of meridional structure in the RMM confounds the MJO signal with equatorial Kelvin waves (Roundy et al., 2009). For these reasons, we use the OMI here.

Following previous MJO predictability studies, we use three metrics for determining MJO predictability: the bivariate anomaly correlation coefficient (ACC), root mean squared error (RMSE) and signal to noise, all of which are calculated using the first two PCs of the ROMI.

2.2.1 ACC and RMSE

Following e.g., Lin et al. (2008), the ACC is calculated as

$$\mathrm{ACC}(t) = \frac{\sum_{i=1}^{N}[a_{1i}(t)b_{1i}(t) + a_{2i}(t)b_{2i}(t)]}{\sqrt{\sum_{i=1}^{N}[a_{1i}^2(t) + a_{2i}^2(t)]}\sqrt{\sum_{i=1}^{N}[b_{1i}^2(t) + b_{2i}^2(t)]}} \tag{1}$$

and root mean squared error (RMSE) as

$$\mathrm{RMSE}(t) = \sqrt{\frac{1}{N}\sum_{i=1}^{N}\left([a_{1i}(t) - b_{1i}(t)]^2 + [a_{2i}(t) - b_{2i}(t)]^2\right)} \tag{2}$$

where $a_{1,2}(t)$ are the two PCs of the ROMI for the control simulation t days after forecast initiation, $b_{1,2}(t)$ are the PCs of the ROMI for the forecast, and N is the number of forecasts. By convention, forecasts are considered skillful until ACC falls below 0.5. The ACC is essentially the weighted similarity of the ROMI, while the RMSE includes information about amplitude differences (Wilks, 2019).

2.2.2 Signal to noise

ACC and RMSE quantify the difference between the control and forecast runs on each day. Another assessment of predictability is to relate the strength of the MJO signal to the day-to-day variability of the tropics (Waliser et al., 2003). As long as the MJO signal remains stronger than the background noise, it could be predictable. We quantify noise as the mean squared error as in previous studies. Since the MJO is a propagating signal with a period of 30-60 days, the "signal" is calculated as the average amplitude of the ROMI within a sliding window that approximately captures a full MJO event. Previous work showed that signal is insensitive to window size, so we follow previous studies and use a 51-day window (Waliser et al., 2003; Neena et al., 2014). Signal is defined as

$$\mathrm{S}^2(t) = \frac{1}{N}\sum_{i=1}^{N}\left(\frac{1}{2L+1}\sum_{t=-L}^{L}[a_{1i}^2(t) + a_{2i}^2(t)]\right) \tag{3}$$

where again $a_{1,2}$ are the two PCs of the control run and L is 25 for a window size of 51. Since the control and forecast runs are essentially separate runs of the same model, we expect signal to be similar if the forecast ROMI was used; we use the control for convenience when calculating the sliding window.

3 Results

To visualize how the MJO simulation differs between the control and forecast runs, we plot the two components of the ROMI on a phase diagram for four example forecasts compared to the control run over the same period (Figure 2). A typical active MJO trajectory will propagate counterclockwise (eastward) outside of the dashed circle (representing an amplitude greater than 1), such as in the two cases on the right in Figure 2. The example forecasts here are chosen arbitrarily to represent forecasts initiated during active MJO periods in Phases 1/8, 2/3, 4/5, and 6/7, but are broadly representative of forecast behavior. The exact timing and pattern differs for each forecast, but in general the control and forecast trajectories track together closely for about 15 days before the amplitude or phase of the forecast run starts to drift from the control. From these examples, we see that the MJO signal remains strongly coherent for at least 10-15 days after the initial convective perturbation in the forecast run.

We use the bivariate ACC and RMSE to quantitatively assess MJO predictability for each day after the forecast initiation (Figure 3). Both metrics are also recalcu-

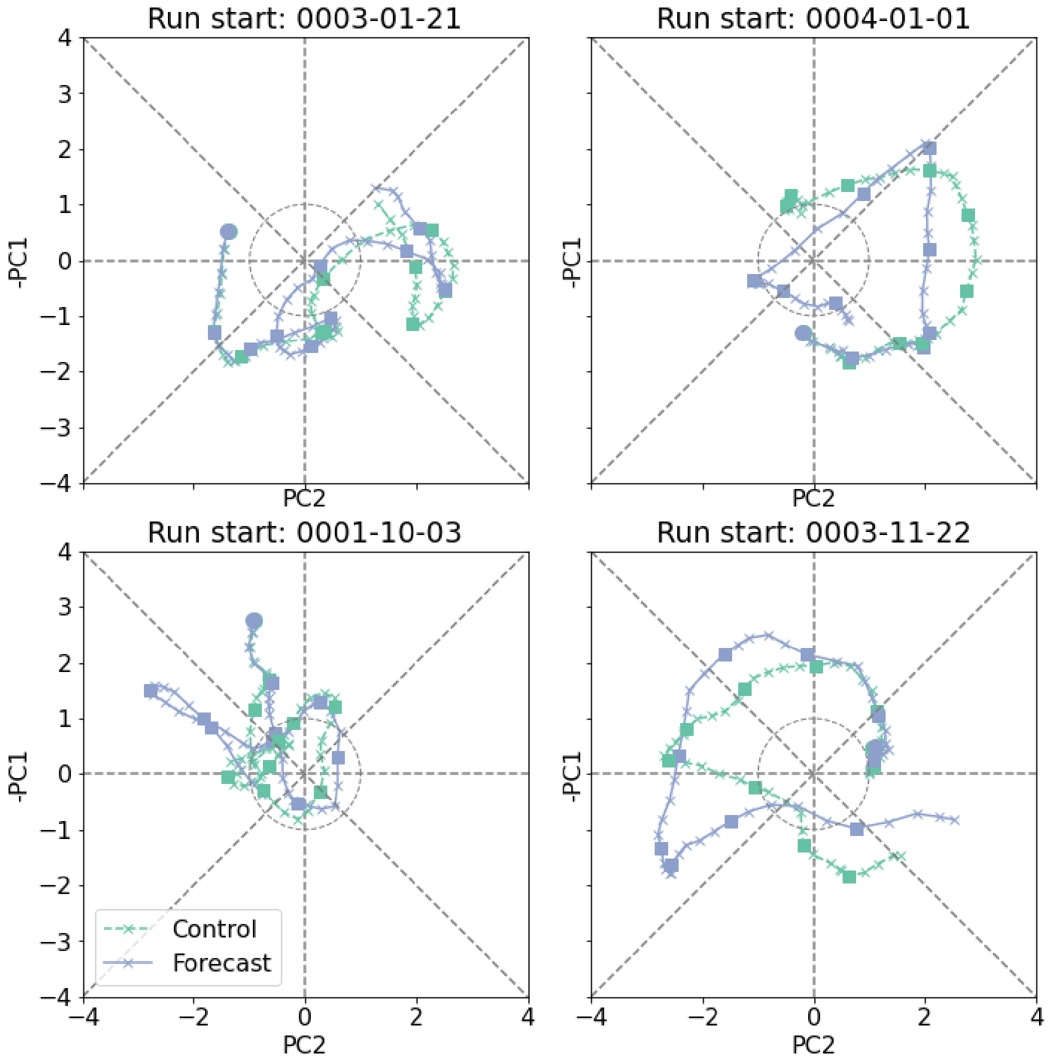

Figure 2. MJO phase trajectories of the ROMI for four example forecast cases. Green dashed lines are the control simulation and purple lines are the forecast runs. Filled circles represent the beginning of the forecast, with squares every subsequent 5 days for a total of 50 days.

lated using only forecasts that were initiated on an active or inactive MJO day as defined by a ROMI amplitude above 1.14, the median amplitude over the 20-year period. The 95% confidence interval is calculated using a Student's t test. The initial strength of the MJO does not significantly affect either of the metrics in Figure 3a,b; the ACC of all three cases fall below 0.5 between days 37-40. The ACC shows nearly perfect correlation for 10-15 days, corroborating the high similarity between the control and forecast trajectories in Figure 2. After the first few days, the RMSE increases approximately linearly until reaching a saturation around days 37-40.

Perhaps a more operationally relevant metric is to look at the predictability of the MJO based on target date; in other words, how far ahead could a strong or weak MJO event be predicted? (Xiang et al., 2015). ACC and RMSE are recalculated based on the strength of the MJO on the target date and shown in Figure 3c,d. A lag of -5 means the forecast was initiated 5 days before a strong or weak MJO target date. The correlation is significantly larger for strong targets compared to weak targets between days 10-30 based on the 95% confidence interval, though they all converge at 0.5 ACC between 37-40 days. The RMSE is about the same for both strong and weak MJO targets until the error saturates after day 40. This is likely because although the correlation is stronger for strong targets, the MJO signal itself (the amplitude of the ROMI) is also larger, so the mean error evens out.

Several studies have suggested that predictability is dependent on target phase of the MJO (S. Wang et al., 2019). ACC is recalculated by separating forecasts by initial phase and target phase using the same methodology as above. Correlations for all initial/target phases and active MJO initial/target phases are plotted in Figure 4. There is little phase dependence in ACC before 20-25 days; afterwards, there is slightly higher predictability for initial phase 2 and target phase 5-6 for all and active MJO periods, and slightly decreased predictability for target phase 2. Phase 2 corresponds to enhanced precipitation over the Indian Ocean, and phase 5-6 aligns with precipitation transitioning from the Maritime Continent to the Western Pacific, generally 15-20 days after phase 2. Several other models have shown worse skill for MJO events that propagate across the Maritime Continent, a phenomenon known as the Maritime Continent barrier (Abhik et al., 2023; Du et al., 2023; S. Wang et al., 2019). SPCAM does not seem to have this problem and in fact finds these events (which are often strong events) more predictable.

Signal and noise (mean squared error) is our final predictability metric (Figure 5). The MJO signal is interpreted as predictable as long as the signal is larger than the error. Again, results seem to be insensitive to strength of initial MJO signal; the signal intersects with error between days 35-40 for all three cases. Since we are using a perfect-model experiment, signal should be nearly constant through lead time; the small increase (decrease) at the beginning of the period for strong (weak) events is because we are restricting our set of forecasts to initially stronger (weaker) MJO signals, and this feature dissipates as the error surpasses the signal. Error slowly increases until it saturates just after surpassing the signal. In general, the signal to noise metric aligns with the conclusions drawn from ACC and RMSE, implying a predictability of the MJO in boreal winter of 35-40 days.

4 Summary and Discussion

By replacing the convective parameterization with a cloud resolving component and using a novel technique to initialize the forecast runs using convective-scale uncertainty, we find the MJO predictability in SPCAM to be about 35-40 days using a single-member ensemble forecast. This estimate is comparable to the highest performing ensemble forecasting models (W. Wang et al., 2014; Xiang et al., 2022; Wu et al., 2016), though these estimates are closer to 20-30 days when using a single-member ensemble forecast as in this study (Neena et al., 2014; H.-M. Kim et al., 2014; Lim et al., 2018). We would ex-

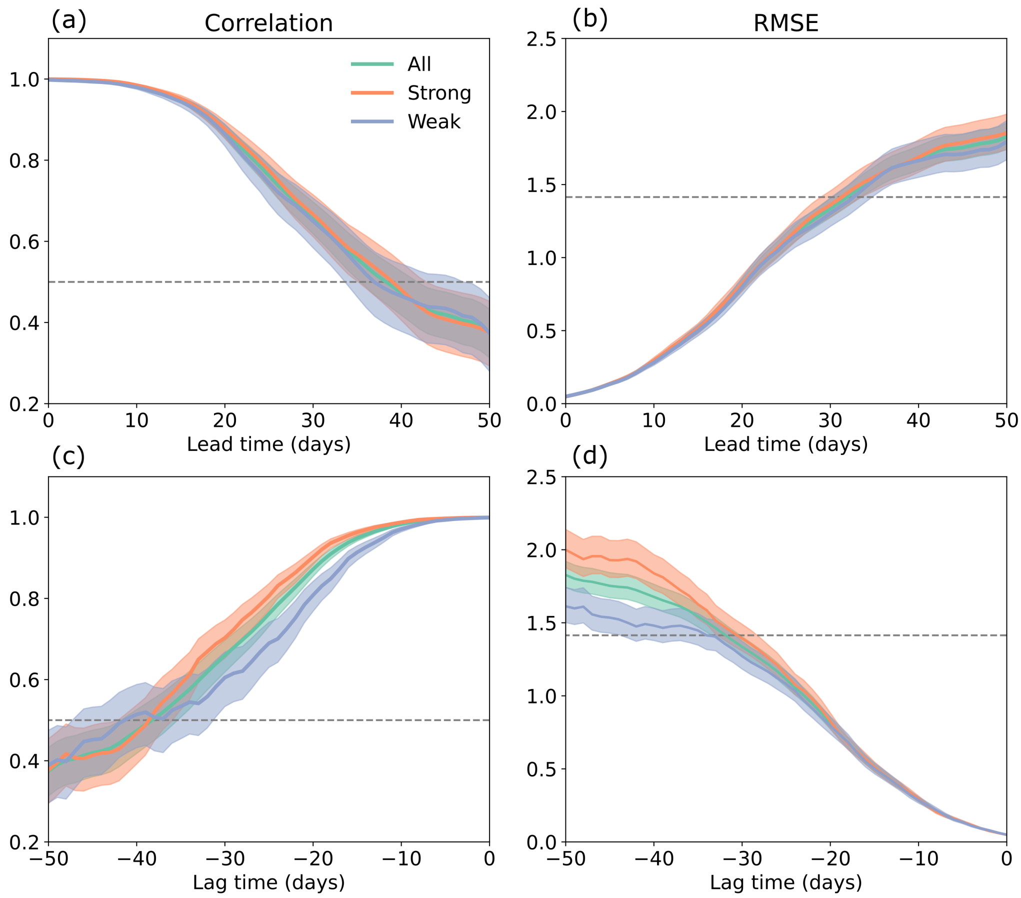

Figure 3. Bivariate anomaly correlation coefficient (left) and RMSE (right) between control and forecast runs by time after forecast initiation. (Top) Using the ROMI principal components at each day, calculated for all forecasts (green), strong MJO initial days (orange) and weak MJO initial days (purple). Shading represents a 95% confidence interval. (Bottom) Same, but using strong and weak target dates. The dashed lines are at 0.5 (left) and $\sqrt{2}$ (right).

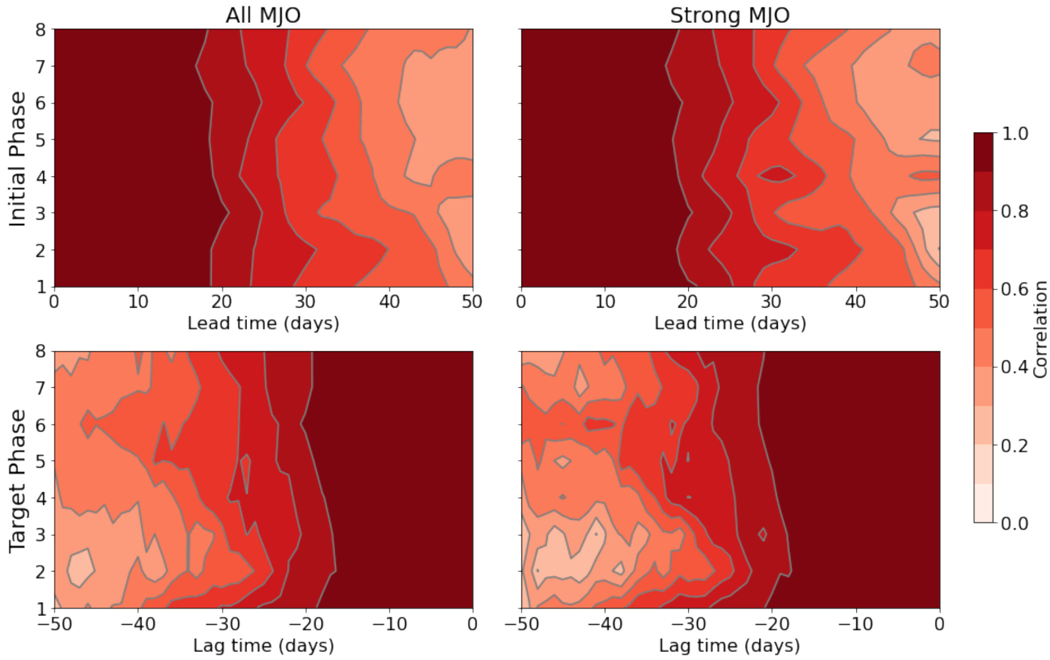

Figure 4. Bivariate ACC by day after forecast initiation, separated by initial (top) and target (bottom) phase of forecast. All forecasts (left) and only strong initial (target) MJO states (right).

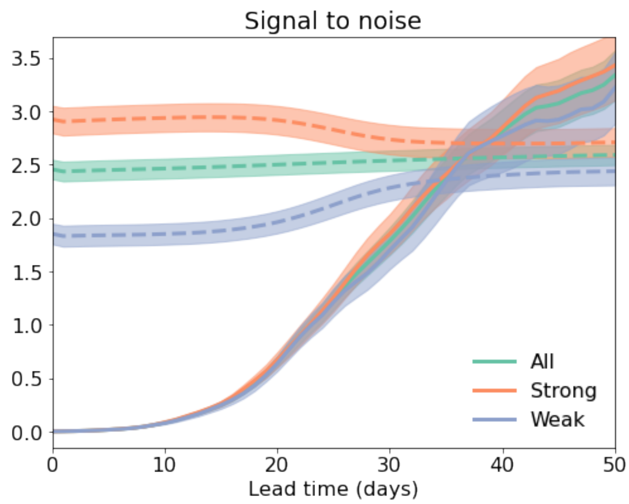

Figure 5. Signal (dashed) to mean squared error (solid) of forecast pairs for all forecasts (green), strong initial days (orange), and weak initial days (purple). Shading represents a 95% confidence interval.

pect an ensemble forecast in SPCAM generated from a set of multiple silent CRMs to increase the estimate of MJO predictability.

MJO predictability in SPCAM is not strongly dependent on initial phase or amplitude, but has slightly higher predictability for strong target dates in phases 5-6. The stronger predictability of MJO events passing over the Maritime Continent is in opposition to most other models whose MJOs tend to dissipate too frequently over the Maritime Continent (S. Wang et al., 2019). Abhik et al. (2023) suggested that this deficiency arises from issues with MJO simulation due to model physics, rather than an inherent predictability barrier. Our results corroborate this hypothesis, since SPCAM more readily simulates MJO propagation across the Maritime Continent and is also biased towards a more active MJO in the Western Pacific.

The potential predictability limits found by SPCAM may not be possible to reach in the real world because the MJO and mean state in SPCAM differ from observations. Since MJO events in SPCAM are in general too vigorous and propagate too easily across the Maritime Continent, our findings may be an overestimation of MJO predictability. Most forecast models have the opposite problem of a weaker and slower MJO than observed, especially over the Western Pacific, all of which would likely result in an underestimation of predictability. The inherent predictability of the real atmosphere may not be properly represented by either approach. In addition, we use prescribed sea surface temperatures, which simplifies the interpretation of the results and reduces computational expense, but restricts our understanding of how MJO predictability is influenced by interactions with different ENSO background states (Mengist & Seo, 2022). Adding an interactive ocean would additionally increase complexity and potential for influences of model bias, but previous studies have shown how including a coupled ocean component can increase predictability of precipitation and OLR after 10 days (Pegion & Kirtman, 2008).

Although it is conventional to use an MJO index to quantify MJO predictability, bivariate indices only capture a condensed slice of actual MJO behavior. The goal of improving MJO forecasts requires an understanding of the phenomenon and the modeling components that are most important for improving those forecasts. This study is a first step in utilizing scale separation in a multiscale model for assessing MJO predictability. With this framework, future work should include a thorough analysis of which physical aspects of the MJO lead to its predictability, or conversely, which aspects of biased MJO simulation in models lead to decreased forecast skill (see potential examples: Du et al. (2023); Liu et al. (2017)). The scale separation in SPCAM also naturally leads to fundamental questions regarding error growth across space and time scales, which would help broaden our understanding of the tropical atmosphere.

5 Open Research

SPCAM is part of the Community Earth System Model project, which is supported primarily by the National Science Foundation (NSF). Information for running SPCAM can be found at `https://wiki.ucar.edu/pages/viewpage.action?pageId=205489281`. The ROMI data and analysis code can be found at `https://doi.org/10.5281/zenodo.8190698`. The EOFs for the ROMI were calculated using the mjoindices Python package published in Hoffmann et al. (2021).

Acknowledgments

S. W. was supported by the NSF GRFP No. DGE 2140743 and Z.K. was supported by NASA grant 80NSSC22K1837. The Harvard Odyssey cluster provided the computing resources for this work. S. W. thanks Qiyu Song for assistance in implementing SPCAM with multiple CRMs. The authors declare no competing interests.

References

Abhik, S., Hendon, H. H., & Zhang, C. (2023, January). The Indo-Pacific Maritime Continent Barrier Effect on MJO Prediction. *Journal of Climate*, *36*(3), 945–957. Retrieved 2023-02-23, from https://journals.ametsoc.org/view/journals/clim/36/3/JCLI-D-22-0010.1.xml (Publisher: American Meteorological Society Section: Journal of Climate) doi: 10.1175/JCLI-D-22-0010.1

Arcodia, M. C., Kirtman, B. P., & Siqueira, L. S. P. (2020, May). How MJO Teleconnections and ENSO Interference Impacts U.S. Precipitation. *Journal of Climate*, *33*(11), 4621–4640. Retrieved 2021-10-22, from http://journals.ametsoc.org/view/journals/clim/33/11/jcli-d-19-0448.1.xml (Publisher: American Meteorological Society Section: Journal of Climate) doi: 10.1175/JCLI-D-19-0448.1

Benedict, J. J., & Randall, D. A. (2009, November). Structure of the Madden–Julian Oscillation in the Superparameterized CAM. *Journal of the Atmospheric Sciences*, *66*(11), 3277–3296. Retrieved 2022-01-31, from https://journals.ametsoc.org/view/journals/atsc/66/11/2009jas3030.1.xml (Publisher: American Meteorological Society Section: Journal of the Atmospheric Sciences) doi: 10.1175/2009JAS3030.1

Du, D., Subramanian, A. C., Han, W., Wei, H.-H., Sarojini, B. B., Balmaseda, M., & Vitart, F. (2023). Assessing the Impact of Ocean In Situ Observations on MJO Propagation Across the Maritime Continent in ECMWF Subseasonal Forecasts. *Journal of Advances in Modeling Earth Systems*, *15*(2), e2022MS003044. Retrieved 2023-07-05, from https://onlinelibrary.wiley.com/doi/abs/10.1029/2022MS003044 (_eprint: https://onlinelibrary.wiley.com/doi/pdf/10.1029/2022MS003044) doi: 10.1029/2022MS003044

Hannah, W. M., Maloney, E. D., & Pritchard, M. S. (2015). Consequences of systematic model drift in DYNAMO MJO hindcasts with SP-CAM and CAM5. *Journal of Advances in Modeling Earth Systems*, *7*(3), 1051–1074. Retrieved 2023-01-24, from https://onlinelibrary.wiley.com/doi/abs/10.1002/2014MS000423 (_eprint: https://onlinelibrary.wiley.com/doi/pdf/10.1002/2014MS000423) doi: 10.1002/2014MS000423

Henderson, S. A., Maloney, E. D., & Barnes, E. A. (2016, June). The Influence of the Madden–Julian Oscillation on Northern Hemisphere Winter Blocking. *Journal of Climate*, *29*(12), 4597–4616. Retrieved 2022-05-25, from https://journals.ametsoc.org/view/journals/clim/29/12/jcli-d-15-0502.1.xml (Publisher: American Meteorological Society Section: Journal of Climate) doi: 10.1175/JCLI-D-15-0502.1

Hoffmann, C. G., Kiladis, G. N., Gehne, M., & von Savigny, C. (2021, May). A Python Package to Calculate the OLR-Based Index of the Madden-Julian-Oscillation (OMI) in Climate Science and Weather Forecasting. *Journal of Open Research Software*, *9*, 9. Retrieved 2022-01-19, from http://openresearchsoftware.metajnl.com/articles/10.5334/jors.331/ doi: 10.5334/jors.331

Jones, T. R., Randall, D. A., & Branson, M. D. (2019). Multiple-Instance Superparameterization: 1. Concept, and Predictability of Precipitation. *Journal of Advances in Modeling Earth Systems*, *11*(11), 3497–3520. Retrieved 2023-04-11, from https://onlinelibrary.wiley.com/doi/abs/10.1029/2019MS001610 (_eprint: https://onlinelibrary.wiley.com/doi/pdf/10.1029/2019MS001610) doi: 10.1029/2019MS001610

Kang, D., Kim, D., Ahn, M.-S., Neale, R., Lee, J., & Gleckler, P. J. (2020). The Role of the Mean State on MJO Simulation in CESM2 Ensemble Simulation. *Geophysical Research Letters*, *47*(24), e2020GL089824. Retrieved 2021-10-22, from http://

onlinelibrary.wiley.com/doi/abs/10.1029/2020GL089824 (_eprint: https://agupubs.onlinelibrary.wiley.com/doi/pdf/10.1029/2020GL089824) doi: 10.1029/2020GL089824

Khairoutdinov, M., DeMott, C., & Randall, D. (2008, February). Evaluation of the Simulated Interannual and Subseasonal Variability in an AMIP-Style Simulation Using the CSU Multiscale Modeling Framework. *Journal of Climate*, *21*(3), 413–431. Retrieved 2023-04-03, from https://journals.ametsoc.org/view/journals/clim/21/3/2007jcli1630.1.xml (Publisher: American Meteorological Society Section: Journal of Climate) doi: 10.1175/2007JCLI1630.1

Khairoutdinov, M., Randall, D., & DeMott, C. (2005, July). Simulations of the Atmospheric General Circulation Using a Cloud-Resolving Model as a Superparameterization of Physical Processes. *Journal of the Atmospheric Sciences*, *62*(7), 2136–2154. Retrieved 2021-10-22, from http://journals.ametsoc.org/view/journals/atsc/62/7/jas3453.1.xml (Publisher: American Meteorological Society Section: Journal of the Atmospheric Sciences) doi: 10.1175/JAS3453.1

Khairoutdinov, M. F., & Randall, D. A. (2001). A cloud resolving model as a cloud parameterization in the NCAR Community Climate System Model: Preliminary results. *Geophysical Research Letters*, *28*(18), 3617–3620. Retrieved 2022-07-20, from https://onlinelibrary.wiley.com/doi/abs/10.1029/2001GL013552 (_eprint: https://onlinelibrary.wiley.com/doi/pdf/10.1029/2001GL013552) doi: 10.1029/2001GL013552

Khairoutdinov, M. F., & Randall, D. A. (2003, February). Cloud Resolving Modeling of the ARM Summer 1997 IOP: Model Formulation, Results, Uncertainties, and Sensitivities. *Journal of the Atmospheric Sciences*, *60*(4), 607–625. Retrieved 2022-11-11, from https://journals.ametsoc.org/view/journals/atsc/60/4/1520-0469_2003_060_0607_crmota_2.0.co_2.xml (Publisher: American Meteorological Society Section: Journal of the Atmospheric Sciences) doi: 10.1175/1520-0469(2003)060⟨0607:CRMOTA⟩2.0.CO;2

Kiladis, G. N., Dias, J., Straub, K. H., Wheeler, M. C., Tulich, S. N., Kikuchi, K., … Ventrice, M. J. (2014, May). A Comparison of OLR and Circulation-Based Indices for Tracking the MJO. *Monthly Weather Review*, *142*(5), 1697–1715. Retrieved 2022-01-19, from https://journals.ametsoc.org/view/journals/mwre/142/5/mwr-d-13-00301.1.xml (Publisher: American Meteorological Society Section: Monthly Weather Review) doi: 10.1175/MWR-D-13-00301.1

Kim, H., Janiga, M. A., & Pegion, K. (2019). MJO Propagation Processes and Mean Biases in the SubX and S2S Reforecasts. *Journal of Geophysical Research: Atmospheres*, *124*(16), 9314–9331. Retrieved 2021-10-22, from http://onlinelibrary.wiley.com/doi/abs/10.1029/2019JD031139 (_eprint: https://agupubs.onlinelibrary.wiley.com/doi/pdf/10.1029/2019JD031139) doi: 10.1029/2019JD031139

Kim, H., Vitart, F., & Waliser, D. E. (2018, December). Prediction of the Madden–Julian Oscillation: A Review. *Journal of Climate*, *31*(23), 9425–9443. Retrieved 2023-02-07, from https://journals.ametsoc.org/view/journals/clim/31/23/jcli-d-18-0210.1.xml (Publisher: American Meteorological Society Section: Journal of Climate) doi: 10.1175/JCLI-D-18-0210.1

Kim, H.-M., Webster, P. J., Toma, V. E., & Kim, D. (2014, July). Predictability and Prediction Skill of the MJO in Two Operational Forecasting Systems. *Journal of Climate*, *27*(14), 5364–5378. Retrieved 2023-02-07, from https://journals.ametsoc.org/view/journals/clim/27/14/jcli-d-13-00480.1.xml (Publisher: American Meteorological Society Section: Journal of Climate) doi: 10.1175/JCLI-D-13-00480.1

Kumar, A., Zhu, J., & Wang, W. (2020, December). Assessing Predictive Potential Associated with the MJO during the Boreal Winter. *Monthly Weather Review*, *148*(12), 4957–4969. Retrieved 2023-02-28, from `https://journals.ametsoc.org/view/journals/mwre/148/12/mwr-d-20-0128.1.xml` (Publisher: American Meteorological Society Section: Monthly Weather Review) doi: 10.1175/MWR-D-20-0128.1

Lim, Y., Son, S.-W., & Kim, D. (2018, May). MJO Prediction Skill of the Subseasonal-to-Seasonal Prediction Models. *Journal of Climate*, *31*(10), 4075–4094. Retrieved 2023-07-26, from `https://journals.ametsoc.org/view/journals/clim/31/10/jcli-d-17-0545.1.xml` (Publisher: American Meteorological Society Section: Journal of Climate) doi: 10.1175/JCLI-D-17-0545.1

Lin, H., Brunet, G., & Derome, J. (2008, November). Forecast Skill of the Madden–Julian Oscillation in Two Canadian Atmospheric Models. *Monthly Weather Review*, *136*(11), 4130–4149. Retrieved 2023-02-07, from `https://journals.ametsoc.org/view/journals/mwre/136/11/2008mwr2459.1.xml` (Publisher: American Meteorological Society Section: Monthly Weather Review) doi: 10.1175/2008MWR2459.1

Liu, X., Wu, T., Yang, S., Li, T., Jie, W., Zhang, L., … Nie, S. (2017, May). MJO prediction using the sub-seasonal to seasonal forecast model of Beijing Climate Center. *Climate Dynamics*, *48*(9), 3283–3307. Retrieved 2023-02-07, from `https://doi.org/10.1007/s00382-016-3264-7` doi: 10.1007/s00382-016-3264-7

Madden, R. A., & Julian, P. R. (1971, July). Detection of a 40–50 Day Oscillation in the Zonal Wind in the Tropical Pacific. *Journal of the Atmospheric Sciences*, *28*(5), 702–708. Retrieved 2022-05-25, from `https://journals.ametsoc.org/view/journals/atsc/28/5/1520-0469_1971_028_0702_doadoi_2_0_co_2.xml` (Publisher: American Meteorological Society Section: Journal of the Atmospheric Sciences) doi: 10.1175/1520-0469(1971)028⟨0702:DOADOI⟩2.0.CO;2

Madden, R. A., & Julian, P. R. (1972, September). Description of Global-Scale Circulation Cells in the Tropics with a 40–50 Day Period. *Journal of the Atmospheric Sciences*, *29*(6), 1109–1123. Retrieved 2022-02-11, from `https://journals.ametsoc.org/view/journals/atsc/29/6/1520-0469_1972_029_1109_dogscc_2_0_co_2.xml` (Publisher: American Meteorological Society Section: Journal of the Atmospheric Sciences) doi: 10.1175/1520-0469(1972)029⟨1109:DOGSCC⟩2.0.CO;2

Mengist, C. K., & Seo, K.-H. (2022). How Long Can the MJO be Predicted During the Combined Phases of ENSO and QBO? *Geophysical Research Letters*, *49*(8), e2022GL097752. Retrieved 2023-06-26, from `https://onlinelibrary.wiley.com/doi/abs/10.1029/2022GL097752` (_eprint: https://onlinelibrary.wiley.com/doi/pdf/10.1029/2022GL097752) doi: 10.1029/2022GL097752

Miyakawa, T., Satoh, M., Miura, H., Tomita, H., Yashiro, H., Noda, A. T., … Yoneyama, K. (2014, May). Madden–Julian Oscillation prediction skill of a new-generation global model demonstrated using a supercomputer. *Nature Communications*, *5*(1), 3769. Retrieved 2023-04-11, from `https://www.nature.com/articles/ncomms4769` (Number: 1 Publisher: Nature Publishing Group) doi: 10.1038/ncomms4769

Neena, J. M., Lee, J. Y., Waliser, D., Wang, B., & Jiang, X. (2014, June). Predictability of the Madden–Julian Oscillation in the Intraseasonal Variability Hindcast Experiment (ISVHE). *Journal of Climate*, *27*(12), 4531–4543. Retrieved 2023-02-07, from `https://journals.ametsoc.org/view/journals/clim/27/12/jcli-d-13-00624.1.xml` (Publisher: American Meteorological Society Section: Journal of Climate) doi: 10.1175/JCLI-D-13-00624.1

Pegion, K., & Kirtman, B. P. (2008, November). The Impact of Air–Sea Interactions on the Predictability of the Tropical Intraseasonal Oscillation. *Jour-*

nal of Climate, *21*(22), 5870–5886. Retrieved 2023-02-07, from https://journals.ametsoc.org/view/journals/clim/21/22/2008jcli2209.1.xml (Publisher: American Meteorological Society Section: Journal of Climate) doi: 10.1175/2008JCLI2209.1

Peng, Y., Liu, X., Su, J., Liu, X., & Zhang, Y. (2023, April). Skill improvement of the yearly updated reforecasts in ECMWF S2S prediction from 2016 to 2022. *Atmospheric and Oceanic Science Letters*, 100357. Retrieved 2023-07-05, from https://www.sciencedirect.com/science/article/pii/S1674283423000351 doi: 10.1016/j.aosl.2023.100357

Randall, D., DeMott, C., Stan, C., Khairoutdinov, M., Benedict, J., McCrary, R., ... Branson, M. (2016, April). Simulations of the Tropical General Circulation with a Multiscale Global Model. *Meteorological Monographs*, *56*(1), 15.1–15.15. Retrieved 2023-04-12, from https://journals.ametsoc.org/view/journals/amsm/56/1/amsmonographs-d-15-0016.1.xml (Publisher: American Meteorological Society Section: Meteorological Monographs) doi: 10.1175/AMSMONOGRAPHS-D-15-0016.1

Roundy, P. E., Schreck, C. J., & Janiga, M. A. (2009, January). Contributions of Convectively Coupled Equatorial Rossby Waves and Kelvin Waves to the Real-Time Multivariate MJO Indices. *Monthly Weather Review*, *137*(1), 469–478. Retrieved 2022-05-25, from https://journals.ametsoc.org/view/journals/mwre/137/1/2008mwr2595.1.xml (Publisher: American Meteorological Society Section: Monthly Weather Review) doi: 10.1175/2008MWR2595.1

Sardeshmukh, P. D., & Hoskins, B. J. (1988, April). The Generation of Global Rotational Flow by Steady Idealized Tropical Divergence. *Journal of the Atmospheric Sciences*, *45*(7), 1228–1251. Retrieved 2022-05-25, from https://journals.ametsoc.org/view/journals/atsc/45/7/1520-0469_1988_045_1228_tgogrf_2_0_co_2.xml (Publisher: American Meteorological Society Section: Journal of the Atmospheric Sciences) doi: 10.1175/1520-0469(1988)045⟨1228:TGOGRF⟩2.0.CO;2

Straub, K. H. (2013, February). MJO Initiation in the Real-Time Multivariate MJO Index. *Journal of Climate*, *26*(4), 1130–1151. Retrieved 2022-05-24, from https://journals.ametsoc.org/view/journals/clim/26/4/jcli-d-12-00074.1.xml (Publisher: American Meteorological Society Section: Journal of Climate) doi: 10.1175/JCLI-D-12-00074.1

Subramanian, A. C., & Palmer, T. N. (2017). Ensemble superparameterization versus stochastic parameterization: A comparison of model uncertainty representation in tropical weather prediction. *Journal of Advances in Modeling Earth Systems*, *9*(2), 1231–1250. Retrieved 2023-01-09, from https://onlinelibrary.wiley.com/doi/abs/10.1002/2016MS000857 (_eprint: https://onlinelibrary.wiley.com/doi/pdf/10.1002/2016MS000857) doi: 10.1002/2016MS000857

Vitart, F. (2014). Evolution of ECMWF sub-seasonal forecast skill scores. *Quarterly Journal of the Royal Meteorological Society*, *140*(683), 1889–1899. Retrieved 2023-07-11, from https://onlinelibrary.wiley.com/doi/abs/10.1002/qj.2256 (_eprint: https://rmets.onlinelibrary.wiley.com/doi/pdf/10.1002/qj.2256) doi: 10.1002/qj.2256

Vitart, F. (2017). Madden—Julian Oscillation prediction and teleconnections in the S2S database. *Quarterly Journal of the Royal Meteorological Society*, *143*(706), 2210–2220. Retrieved 2023-04-04, from https://onlinelibrary.wiley.com/doi/abs/10.1002/qj.3079 (_eprint: https://onlinelibrary.wiley.com/doi/pdf/10.1002/qj.3079) doi: 10.1002/qj.3079

Vitart, F., & Robertson, A. W. (2018, March). The sub-seasonal to seasonal prediction project (S2S) and the prediction of extreme events. *npj Cli-*

mate and Atmospheric Science, *1*(1), 1–7. Retrieved 2023-07-05, from https://www.nature.com/articles/s41612-018-0013-0 (Number: 1 Publisher: Nature Publishing Group) doi: 10.1038/s41612-018-0013-0

Waliser, D. E., Lau, K. M., Stern, W., & Jones, C. (2003, January). Potential Predictability of the Madden–Julian Oscillation. *Bulletin of the American Meteorological Society*, *84*(1), 33–50. Retrieved 2023-02-06, from https://journals.ametsoc.org/view/journals/bams/84/1/bams-84-1-33.xml (Publisher: American Meteorological Society Section: Bulletin of the American Meteorological Society) doi: 10.1175/BAMS-84-1-33

Wang, B., Chen, G., & Liu, F. (2019, July). Diversity of the Madden-Julian Oscillation. *Science Advances*, *5*(7), eaax0220. Retrieved 2022-07-18, from https://www.science.org/doi/10.1126/sciadv.aax0220 (Publisher: American Association for the Advancement of Science) doi: 10.1126/sciadv.aax0220

Wang, S., Sobel, A. H., Tippett, M. K., & Vitart, F. (2019, May). Prediction and predictability of tropical intraseasonal convection: seasonal dependence and the Maritime Continent prediction barrier. *Climate Dynamics*, *52*(9), 6015–6031. Retrieved 2022-05-25, from https://doi.org/10.1007/s00382-018-4492-9 doi: 10.1007/s00382-018-4492-9

Wang, W., Hung, M.-P., Weaver, S. J., Kumar, A., & Fu, X. (2014, May). MJO prediction in the NCEP Climate Forecast System version 2. *Climate Dynamics*, *42*(9), 2509–2520. Retrieved 2023-03-28, from https://doi.org/10.1007/s00382-013-1806-9 doi: 10.1007/s00382-013-1806-9

Weidman, S., Kleiner, N., & Kuang, Z. (2022). A Rotation Procedure to Improve Seasonally Varying Empirical Orthogonal Function Bases for MJO Indices. *Geophysical Research Letters*, *49*(15), e2022GL099998. Retrieved 2023-03-15, from https://onlinelibrary.wiley.com/doi/abs/10.1029/2022GL099998 (_eprint: https://onlinelibrary.wiley.com/doi/pdf/10.1029/2022GL099998) doi: 10.1029/2022GL099998

Wheeler, M. C., & Hendon, H. H. (2004, August). An All-Season Real-Time Multivariate MJO Index: Development of an Index for Monitoring and Prediction. *Monthly Weather Review*, *132*(8), 1917–1932. Retrieved 2022-01-19, from http://journals.ametsoc.org/view/journals/mwre/132/8/1520-0493_2004_132_1917_aarmmi_2.0.co_2.xml (Publisher: American Meteorological Society Section: Monthly Weather Review) doi: 10.1175/1520-0493(2004)132⟨1917:AARMMI⟩2.0.CO;2

Wilks, D. S. (2019). Part ii - Univariate Statistics. In D. S. Wilks (Ed.), *Statistical Methods in the Atmospheric Sciences (Fourth Edition)* (Fourth Edition ed., p. 23-550). Elsevier. Retrieved from https://www.sciencedirect.com/science/article/pii/B9780128158234099879 doi: https://doi.org/10.1016/B978-0-12-815823-4.09987-9

Wu, J., Ren, H.-L., Jia, X., & Zhang, P. (2023). Climatological diagnostics and subseasonal-to-seasonal predictions of Madden–Julian Oscillation events. *International Journal of Climatology*, *43*(5), 2449–2464. Retrieved 2023-06-27, from https://onlinelibrary.wiley.com/doi/abs/10.1002/joc.7984 (_eprint: https://rmets.onlinelibrary.wiley.com/doi/pdf/10.1002/joc.7984) doi: 10.1002/joc.7984

Wu, J., Ren, H.-L., Zuo, J., Zhao, C., Chen, L., & Li, Q. (2016, September). MJO prediction skill, predictability, and teleconnection impacts in the Beijing Climate Center Atmospheric General Circulation Model. *Dynamics of Atmospheres and Oceans*, *75*, 78–90. Retrieved 2023-02-15, from https://www.sciencedirect.com/science/article/pii/S0377026516300392 doi: 10.1016/j.dynatmoce.2016.06.001

Xiang, B., Harris, L., Delworth, T. L., Wang, B., Chen, G., Chen, J.-H., … Zhou, X. (2022, February). S2S Prediction in GFDL SPEAR: MJO Diversity and Teleconnections. *Bulletin of the American Meteorological Society*, *103*(2), E463–E484. Retrieved 2022-07-14, from https://journals.ametsoc.org/view/journals/bams/103/2/BAMS-D-21-0124.1.xml (Publisher: American Meteorological Society Section: Bulletin of the American Meteorological Society) doi: 10.1175/BAMS-D-21-0124.1

Xiang, B., Zhao, M., Jiang, X., Lin, S.-J., Li, T., Fu, X., & Vecchi, G. (2015, July). The 3–4-Week MJO Prediction Skill in a GFDL Coupled Model. *Journal of Climate*, *28*(13), 5351–5364. Retrieved 2023-07-05, from https://journals.ametsoc.org/view/journals/clim/28/13/jcli-d-15-0102.1.xml (Publisher: American Meteorological Society Section: Journal of Climate) doi: 10.1175/JCLI-D-15-0102.1

Zavadoff, B. L., Gao, K., Lopez, H., Lee, S.-K., Kim, D., & Harris, L. M. (2023). Improved MJO Forecasts Using the Experimental Global-Nested GFDL SHiELD Model. *Geophysical Research Letters*, *50*(6), e2022GL101622. Retrieved 2023-06-26, from https://onlinelibrary.wiley.com/doi/abs/10.1029/2022GL101622 (_eprint: https://onlinelibrary.wiley.com/doi/pdf/10.1029/2022GL101622) doi: 10.1029/2022GL101622

Zhu, H., Hendon, H., & Jakob, C. (2009, September). Convection in a Parameterized and Superparameterized Model and Its Role in the Representation of the MJO. *Journal of the Atmospheric Sciences*, *66*(9), 2796–2811. Retrieved 2023-02-22, from https://journals.ametsoc.org/view/journals/atsc/66/9/2009jas3097.1.xml (Publisher: American Meteorological Society Section: Journal of the Atmospheric Sciences) doi: 10.1175/2009JAS3097.1

Zhu, J., Kumar, A., & Wang, W. (2020, May). Dependence of MJO Predictability on Convective Parameterizations. *Journal of Climate*, *33*(11), 4739–4750. Retrieved 2023-02-22, from https://journals.ametsoc.org/view/journals/clim/33/11/jcli-d-18-0552.1.xml (Publisher: American Meteorological Society Section: Journal of Climate) doi: 10.1175/JCLI-D-18-0552.1